



A Model for Designing Adaptive Laboratory Evolution Experiments

LaCroix, Ryan A.; Palsson, Bernhard O.; Feist, Adam M.; Kivisaar, Maia

Published in:
Applied and Environmental Microbiology

Link to article, DOI:
[10.1128/AEM.03115-16](https://doi.org/10.1128/AEM.03115-16)

Publication date:
2017

Document Version
Peer reviewed version

[Link back to DTU Orbit](#)

Citation (APA):
LaCroix, R. A., Palsson, B. O., Feist, A. M., & Kivisaar, M. (Ed.) (2017). A Model for Designing Adaptive Laboratory Evolution Experiments. *Applied and Environmental Microbiology*, 83(8), [e03115-16].
<https://doi.org/10.1128/AEM.03115-16>

General rights

Copyright and moral rights for the publications made accessible in the public portal are retained by the authors and/or other copyright owners and it is a condition of accessing publications that users recognise and abide by the legal requirements associated with these rights.

- Users may download and print one copy of any publication from the public portal for the purpose of private study or research.
- You may not further distribute the material or use it for any profit-making activity or commercial gain
- You may freely distribute the URL identifying the publication in the public portal

If you believe that this document breaches copyright please contact us providing details, and we will remove access to the work immediately and investigate your claim.

1 A Model for Designing Adaptive Laboratory Evolution Experiments

2 Ryan A. LaCroix¹, Bernhard O. Palsson^{1,2,3}, Adam M. Feist^{1,2}

3

4 ¹ Department of Bioengineering, University of California, San Diego, California, United States

5 ² Novo Nordisk Foundation Center for Biosustainability, Technical University of Denmark,
6 Lyngby, Denmark

7 ³ Department of Pediatrics, University of California, San Diego, California, United States

8

9 Running Head: Designing Adaptive Laboratory Evolution Experiments

10

11 Address correspondence to Adam M. Feist, afeist@ucsd.edu

12 **Abstract**

13 The occurrence of mutations is a cornerstone of the evolutionary theory of adaptation,
14 capitalizing on the rare chance that a mutation confers a fitness benefit. Natural selection is
15 increasingly being leveraged in laboratory settings for industrial and basic science applications.
16 Despite an increasing deployment, there are no standardized procedures available for designing
17 and performing adaptive laboratory evolution (ALE) experiments. Thus, there is a need to
18 optimize the experimental design, specifically for determining when to consider an experiment
19 complete and for balancing outcomes with available resources (i.e., lab supplies, personnel, and
20 time). To design and better understand ALE experiments, a simulator, ALEsim, was developed,
21 validated, and applied to optimize ALE experimentation. The effects of various passage sizes
22 were experimentally determined and subsequently evaluated with ALEsim to explain differences
23 in experimental outcomes. Further, a beneficial mutation rate of $10^{-6.9}$ - $10^{-8.4}$ mutations per cell
24 division was derived. A retrospective analysis of ALE experiments revealed that passage sizes
25 typically employed in serial passage batch culture ALE experiments led to inefficient production
26 and fixation of beneficial mutations. ALEsim and the results herein will aid in the design of ALE
27 experiments to fit the exact needs of the project while taking into account the tradeoff in
28 resources required, and lower the barrier of entry to this experimental technique.

29

30 Importance

31 Adaptive laboratory evolution (ALE) is a widely used scientific technique to increase scientific
32 understanding, as well as create industrially relevant organisms. The manner in which ALE
33 experiments are conducted is highly manual and uniform with little optimization for efficiency.
34 Such inefficiencies result in suboptimal experiments that can take multiple months to complete.
35 With the availability of automation and computer simulations, we can now perform these
36 experiments in a more optimized fashion and design experiments to generate greater fitness in a
37 more accelerated time frame, thereby pushing the limits of what adaptive laboratory evolution
38 can achieve.

39

40 Highlights

- 41 - A tunable simulator, ALEsim, was constructed to simulate observed fitness increases in
42 ALE experiments
- 43 - A control ALE experiment was performed to determine an observed beneficial mutation
44 rate and quantify the effect of passage size in an ALE experiment – the beneficial
45 mutation rate (BMR) is consistent with previous estimates
- 46 - A retrospective analysis of ALE experiments revealed limitations in experimental
47 designs.
- 48 - ALEsim can be leveraged to optimize resources and time needed to conduct an ALE
49 experiment by determining tradeoffs between a likely fitness increase and an increased
50 run time

51

52 Introduction

53 Adaptive laboratory evolution (ALE) has been performed *in vitro* for decades and the field is
54 expanding. ALE involves subjecting a population of organisms to a given environment, in the
55 lab, and allowing natural selection to increase the overall fitness of the population. In laboratory
56 settings, this is typically performed with organisms possessing short generation times. The basic
57 principles governing ALE experiments are easily understood across a breadth of disciplines,
58 which has led to its adoption in many laboratories (1, 2). The recent growth in the use of ALE
59 can be attributed to the ease of access and decreasing costs of genome sequencing (3-5). Falling
60 sequencing costs have led to the increased investigation of genomic, transcriptomic, and
61 additional omics data types over the course of evolution (5). While the analysis of ALE
62 experiments has grown, the manner in which the ALE experiments themselves are performed has
63 remained relatively *ad hoc*. The most commonly employed techniques are chemostat adaptation
64 and serially passaged batch culture adaptation, with batch culture adaptation being more popular
65 as it is easily expanded and does not require setting up complex machinery (3, 6).

66 A primary attribute of any ALE experiment is the selection pressure imposed on the culture. The
67 selection pressure (i.e., exponential growth, biomass yield, stationary phase, or lag phase) is
68 responsible for the outcome of the evolution study (4, 7-10). For example, in a 24hr serially
69 passaged batch culture ALE experiment with fast growing bacteria, the culture is subjected to
70 alternating environments of feast and famine. At the beginning of each batch there are excess
71 nutrients but inevitably, within 24hrs, the nutrients are consumed and stationary phase is reached.
72 Because of this alternating environment, the selection pressure is complex and fitness is achieved
73 through various methods (e.g., stationary phase fitness, lag phase duration, and growth rate all
74 contribute) (9). This complexity often confounds the analysis depending on the application. To

75 alleviate complexity, the cells can be kept in one phase (e.g. exponential phase) to mitigate most
76 of the alternating selection and focus selection specifically on fitness gains through growth rate.
77 In such cases, fitness will be treated as interchangeable with growth rate. The desired outcome of
78 the experiment would dictate the ideal selection pressure to be imposed and thereby the
79 experimental design, but the difference between the two designs is non trivial.

80 There are several parameters that affect the outcome of a serially passaged batch culture ALE
81 experiment. A primary parameter involved is the passage size (11-13). Specifically, passage size
82 determines how much of the population is allowed to propagate to each subsequent batch culture.
83 If a beneficial mutation occurs, but is lost when the bottleneck is imposed, the rate of evolution
84 can be slowed or even halted. Since smaller passage sizes can hinder the rate of evolution, it is
85 often easier to perform a serially passaged batch culture ALE under alternating environments of
86 feast and famine where a change in passage size only effects the duration of growth and
87 stationary phases. However, if the application requires exponential phase passaging, a change in
88 passage size also changes the time when the culture must be passaged. Because of this, the
89 passage size is often dictated by an individual's schedule. Typically, the time in between
90 passaging can be no shorter than ~12hrs. Consequentially, as the culture adapts and begins to
91 grow faster, the passage size must be decreased. As an example, a previous study adapting *E.*
92 *coli* to glycerol in 250mL batches started with a passage size of approximately 100 μ L and by
93 experiment's end was less than 0.1 μ L (14). A more in-depth retrospective analysis revealed
94 similar trends where passage amounts were significantly decreased (14-18). In these studies, the
95 reduction in population size, or bottleneck, (i.e., passage size) became so significant that the
96 calculated number of cells being passed was on the order of 10 or even occasionally 1. The
97 chance of capturing a beneficial mutation, when only passing tens of cells from a culture of

98 millions, is practically null over a reasonable timeframe. At this point, continuing the experiment
99 is futile. The question then becomes at what point is the passage size too low?

100 Passage size can have a large impact on the trajectory of an ALE experiment. This can be seen in
101 the comparison of two studies that evolved wild-type *E. coli* K-12 MG1655 on M9 glucose
102 minimal media (7, 18). One study (7) used a consistent passage size of 800 μ L from 25mL
103 batches on an automated platform. The second study (18) was done “by hand” and had widely
104 varying passage sizes that were considerably smaller than the automated study. The outcomes of
105 the ALE experiments were quite distinct. The final growth rates achieved were $1.00 \pm 0.24 \text{ hr}^{-1}$
106 and $0.79 \pm 0.01 \text{ hr}^{-1}$ in the consistent and variable passage size studies, respectively. The apparent
107 lack of fitness achieved in variable passage study was not due to a lack of available beneficial
108 mutations (as the same strains and culturing conditions were used), but rather insufficient
109 experimental design to find and fix them in a reasonable amount of time. Understanding why
110 these two outcomes differ is imperative to the efficient design of ALE experiments.

111 Theoretical studies have looked at the effect of passage size on serially passaged batch culture
112 adaptation and resulted in varying predictions of an ideal passage size depending on the model
113 used (19, 20). The ideal passage sizes calculated are ideal from a mathematical standpoint. This
114 essentially gives the best chance for various mutations of different selective advantages to fix in
115 a population. The ideal passage sizes calculated in these studies are relatively large (13.5% and
116 20%)(19, 20). As mentioned previously, a larger passage necessitates an increase in resources.
117 More specifically, the resources required increase exponentially with passage size, yet the gains
118 slowly diminish. This work thus focuses on examining the diminishing returns in the context of
119 the desired result and the resources available. We set out to examine the impact of the key ALE
120 parameter: passage size. To address this, we created an *in silico* evolutionary model that

121 simulates the dynamics of capturing and fixing beneficial mutations in the context of an
122 exponentially-passed batch culture ALE experiment. After building the model, we parameterize
123 it using a combination of 30 independent ALE experiments of *E. coli* on glycerol minimal media
124 across five different passage sizes (10%, 1%, 0.1%, 0.01%, and 0.001%). Using the
125 parameterized model, we investigated the biological consequences of changing passage sizes and
126 how close to optimal a given experiment is. With this knowledge, an experiment can be designed
127 to fit the desired outcome, giving consideration to the resources required to achieve it, and the
128 feasibility of performing such an experiment.

129

130 **Materials and Methods**

131 **Adaptive Laboratory Evolution**

132 Adaptive laboratory evolutions were started from wild-type *E. coli* strain MG1655
133 (ATCC47076) glycerol frozen stock and grown up overnight in 15mL magnetically stirred 0.2%
134 glycerol M9 minimal media supplemented with trace elements. The magnet was stirred at
135 1150rpm, sufficient for completely aerobic growth. 30 experiments were started from 150μL
136 aliquots from the overnight pre-culture. The experiments were subsequently grown in identical
137 vessels and media as the pre-culture. Culture optical densities at 600nm (OD) were monitored
138 over the course of each batch culture. When the culture reached an OD of 0.300 ($\pm 10\%$) as
139 measured by a plate-reader with 100μL sample volume in a 96 well flat bottom microplate, an
140 aliquot was taken and passed to a new batch culture filled with sterile media. An OD of 0.300
141 was chosen to preclude reaching stationary phase in any of the cultures and ensures OD
142 measurements have not begun to saturate. Growth rates of each culture were determined using
143 OD measurements taken over the lifetime of each batch culture.

144 **Media**

145 All cultures were grown in 0.2% glycerol M9 minimal media. The media consisted of 0.2%
146 glycerol by volume, 0.1mM CaCl₂, 2.0mM MgSO₄, Trace element solution and M9 salts. 4000X
147 Trace element solution consisted of 27g/L FeCl₃*6H₂O, 2g/L ZnCl₂*4H₂O, 2g/L CoCl₂*6H₂O,
148 2g/L NaMoO₄*2H₂O, 1g/L CaCl₂*H₂O, 1.3g/L CuCl₂*6H₂O, 0.5g/L H₃BO₃, and Concentrated
149 HCl dissolved in ddH₂O and sterile filtered. 10x M9 Salts solution consisted of 68g/L Na₂HPO₄
150 anhydrous, 30g/L KH₂PO₄, 5g/L NaCl, and 10g/L NH₄Cl dissolved ddH₂O and autoclaved. Final
151 concentrations in the media were 1x.

152 DNA Sequencing

153 Genomic DNA was isolated using Macherey-Nagel NucleoSpin® Tissue kit. The quality of
154 DNA was assessed with UV absorbance ratios using a Nano drop. DNA was quantified using
155 Qubit dsDNA High Sensitivity assay. Paired-end resequencing libraries were generated using
156 Illumina's Nextera XT kit with 700 pg of input DNA total. Sequences were obtained using an
157 Illumina Miseq with a MiSeq 600 cycle reagent kit v3. The breseq pipeline version 0.23 with
158 bowtie2 was used to map sequencing reads and identify mutations relative to the *E. Coli* K12
159 MG1655 genome (NCBI accession NC_000913.2) (21). All samples had an average mapped
160 coverage of at least 25x.

161 Computer Modeling

162 Modeling of simulations was computed using MATLAB 2015b on a Windows 7 professional
163 platform. Detailed descriptions are found as comments in the supplemental m-files. The
164 beneficial mutation rate was computed by a maximum likelihood estimation. It was calculated
165 for making a transition from State 1 to State 2 and State 2 to State 3 for passage sizes of 0.01%
166 and 0.001%. These passage size were chosen as they were the only ones that showed a
167 distribution of states achieved. The transition from State 1 to State 2 was capped at 20 days to
168 give a maximally distributed data set. The transition from State 2 to State 3 was started by
169 assuming that State 2 was already achieved. Thus, the length of time simulated was started based
170 of when State 2 was achieved. This was variable for different experiments.

171 A value of 1.55×10^{12} cells \cdot L⁻¹ \cdot OD_{600nm}⁻¹ was used to estimate the number of cells in a culture
172 for a given OD_{600nm} with a 1 cm path length cuvette for the purposes of ALEsim. A standard
173 curve relating the ODs measured in the plate reader with a 100 μ L sample volume in a 96 well

174 flat bottom microplate to the OD measured with a 1 cm cuvette to obtain a ratio of 3.15 for
175 equivalent measurements between the two. The biomass (grams of dry weight) per OD_{600nm} per
176 volume was calculated by filtering known volumes of cultures at specific ODs through 0.22µm
177 filters. The filters were weighed before and after filtering and drying to obtain the total dry
178 weight of the culture. The differences in these values was used to calculate ratio of 0.45·gDW L⁻¹
179 $\cdot \text{OD}_{600\text{nm}}^{-1}$. The dry mass per cell has previously been reported as 2.9×10^{-13} gDW·cell (22). The
180 quotient of these two values gives our final conversion factor of 1.55×10^{12} cells·L⁻¹·OD⁻¹ to
181 estimate the cell counts of cultures at various ODs and volumes. . For *E. coli*, the dry mass per
182 cell can vary over a range of growth rates (23). Using such a variable OD to cell count factor as a
183 function of growth rate is possible with ALEsim, but incurs a marked increase in simulation
184 time. Thus, identical simulations were performed using only the highest and lowest dry mass per
185 cell values expected for the growth rates observed (i.e., the extremes). Only a 10% difference in
186 the distribution of simulated endpoint growth rates were observed between the two extremes (see
187 Supplementary Figure S1). Therefore, use of a constant average value for dry mass per cell over
188 the range of growth rates expected was determined to be sufficient considering the benefit in
189 computation time.

190 Although possible with ALEsim, deleterious and neutral mutations were not considered during
191 this study. A deleterious mutation rate of 1 in 5,000 was previously computed (24). In the
192 application demonstrated here, the population sizes were sufficiently large ($10^5 - 10^9$ cells) such
193 that the effects of deleterious and neutral mutations would be negligible. With smaller population
194 sizes (e.g., several orders of magnitude smaller than the population sizes modeled here), the
195 effects of these mutations become more pronounced and should not be ignored.

196

197 Results

198 Modeling the ALE process

199 ALEsim is a model built on the basic principles of exponential growth in order to understand the
200 dynamics of ALE. The scope of ALEsim is to predict the observed growth rate in each batch
201 culture of an ALE experiment while allowing individual cells to change their growth rate when
202 dividing (i.e., a proxy for receiving a beneficial mutation). This preferentially finds only those
203 beneficial mutations that fix. There is a likely chance that other beneficially mutations are
204 unobserved due to clonal interference. The observed population growth rate is different from a
205 clonal growth rate in that each batch culture of an ALE experiment is a population of multiple
206 clones with varying growth rates. Figure 1 provides a workflow of the modeling process and the
207 full details are in Supplementary File ALEsim.txt. Each *in silico* experiment begins with a clonal
208 inoculation of a strain with a given growth rate. A population of mixed phenotypes can be used
209 in this framework, but here the starting population will be assumed to be isogenic with the same
210 phenotypic behavior. This organism is allowed to replicate according to an exponential growth
211 function. During each cell division event, there is a probability that it will mutate and start a new
212 lineage with a mutated growth rate. This new lineage is allowed to grow alongside the parent
213 strain according to exponential growth, but with its mutated growth rate. The new lineage is
214 itself allowed to continue mutating in the simulation.

215 Mutated growth rates in ALEsim must be constrained to remain biologically meaningful, i.e.,
216 growth rates that are of magnitudes that remain plausible. These rates are determined empirically
217 by the user, as done here from the parameterization experiment (see section below). The growth
218 rates can be constrained to allow various types of epistasis. For example, if two distinct growth
219 rates are allowed, there is a possibility that a single cell line could mutate twice and receive both

220 of these mutations. ALEsim employs the flexibility to define the type of epistasis between these
221 two mutations, if any epistasis at all is to occur. Similarly, an order to the mutations accumulated
222 can be set, as certain mutations can be beneficial only in the presence of a pre-existing mutation
223 (i.e., epistasis can be modeled). As the population of cells continues to replicate and mutate, their
224 total cell count naturally increases. When the cell count reaches a given threshold, a simple
225 random sample of cells is used to inoculate the next batch culture. The threshold corresponds to a
226 target cell count at which to passage the cells to the next batch culture. The number of cells taken
227 is determined by the passage size, which is a percentage of the total culture volume. After this
228 sample is computed, a new batch culture is started with the chosen cells and corresponding
229 growth rates. Figure 2 provides the key parameters of the model.

230 In using the basic principles of microbial growth and a brute force computational approach,
231 many of the fundamental attributes of natural selection are intrinsically contained in the
232 simulation. This includes clonal interference which is pervasive to asexual evolution. ALEsim
233 can be used to model a system where two local maxima are possible but the greater maximum
234 can only be found by first acquiring a mutation that is initially suboptimal compared to other
235 possible single beneficial mutations (25). How to achieve this is shown in the model
236 documentation (ALEsim.txt). The experimental parameters can be modulated to potentially find
237 an experiment design that would find the desired optimum or both.

238 Given the stochastic nature of many steps in the model, the results are non-deterministic.
239 Stochasticity is incorporated into the model in three ways: i) when a cell mutates its growth rate,
240 ii) what growth rate a cell mutates to, and iii) what sample of cells are propagated to a
241 subsequent batch culture. The simulation is then run multiple times to capture the dynamics of
242 the stochasticity (26).

243 For a simulation to be biologically meaningful using the developed model, there are three types
244 of parameter sets that must be determined. The first set of parameters is experimental: batch
245 culture size, passage size, passage optical density (or cell count), and length of experiment.
246 These can be set based on the desired experimental setup.(23) The second set is the statistical
247 parameters: random number seed and the number of identical experiments to run. The random
248 number seed is set by the native random number generator. The number of parallel simulations to
249 run is determined by the statistical power needed. Depending on the magnitudes and
250 complexities of the parameters set, the number of simulations can vary drastically. For the results
251 shown here, 500 simulations were computed unless otherwise stated. It was found that after 500
252 simulations there was no appreciable difference in the means or spread of the distribution of
253 results calculated when combined with another set of 500. The third set of parameters is
254 biological: beneficial mutation rate (BMR) and allowed increases in growth rate. These
255 parameters are defined in the models and can be constrained by any method that can be
256 expressed programmatically, whether this it is randomly decided within a meaningful range or
257 set to distinct values. This set of parameters must be derived experimentally. Intuitively, these
258 parameters can be different for different strains, conditions, and can even change along the
259 course of a single experiment (27, 28). As long as the values determined are biologically
260 meaningful, generalizations about the ALE process can be concluded.

261 Alternative models of evolution and adaption have been developed to understand the dynamics
262 of evolution. These types of mathematical models capture various aspects of adaptation
263 including selection, drift, and clonal interference (29-31). Classically, this has been a target of
264 the field of population genetics (32-34). An expansion of the Fisher model was developed by
265 Wahl et. al. which conceptually relates to ALEsim in that it targets the question of passage sizes

(35). However, ALEsim deviates from the classical mathematical approach and employs the use of an *in silico* organism that can then replicate, mutate, and evolve. Simulations here are carried out in brute force where they are allowed to grow under the conditions laid out by the user. The advantage of such a method is that the experimental and biological parameters can be strictly controlled over the course of an experiment. The resulting simulation is able to more closely mimic the conditions of an actual laboratory evolution experiment in its entirety where parameters are not always constant throughout. This approach differs from the use of a digital organism in that it is an attempt to model specific biology instead of general evolutionary dynamics which allows for direct modeling of the ALE experiment as would be performed in a laboratory (36).

Parameterization of ALEsim by evolving *E. coli* on Glycerol Minimal Media

The two biological parameters, the beneficial mutation rate and allowed increase in growth rate, were determined using 30 independent cultures of *Escherichia coli* K-12 MG1655 evolved in 15mL of 0.2% glycerol M9 minimal media until a stable growth rate was observed in most experiments (38 days). One experiment only lasted 23 days after it was restarted due to contamination. The 30 experiments were separated into five groups of six passage sizes and each group was evolved under identical conditions except for the passage size. The passage sizes used were 10%, 1%, 0.1%, 0.01%, and 0.001% of the culture size (15mL). The growth rate of each experiment was monitored over the course of the experiment using optical density measurements as a proxy for cell count (Figure 3). Fitness related details can be found in the supplement (Supplementary Table 1 and Supplementary File fitness_data.xlsx).

Allowed increases in growth rate were determined by identifying jumps in growth rates from the fitness trajectories. A spline was fit to the growth rate of each experiment and significant

289 increases in growth rate were identified as discussed previously (7). The resulting jumps in
290 growth rates showed that the plateaus in growth occurred at specific values (Figure 3, 4). These
291 plateaus are identified as State 1, 2, 3A, and 3B. State 3 was split into two sub-states since there
292 is a significant difference between those in state 3A and 3B (Wilcoxon rank sum $p < 0.01$),
293 however there exists no identifiable increase in growth rate or gap between states that would
294 characterize this transition. This gap is most likely obscured since the difference between the
295 growth rates is fairly small and noise in the measurements can bleed into any gap that might
296 exist. Figure 4 groups the jumps in fitness observed by their transition between states. Contrary
297 to the conclusion of other ALE experiments, the largest jump in fitness was not observed first but
298 actually followed a smaller jump. This yields an allowed increase in growth rate that can be used
299 to constrain ALEsim. In simulations run here, the growth rates allowed were set to the mean of
300 the range of each state.

301 The beneficial mutation rate (BMR) can be calculated by fitting ALEsim to the distribution of
302 the end states. Passage sizes of 10% - 0.1% did not show any appreciable variation between
303 states, thus only the experiments with passage sizes of 0.01% and 0.001% were used for fitting.
304 ALEsim was fit by performing simulations that only allowed for a single jump from one state to
305 another. Multi-state jumps and two sequential jumps were not allowed. This simplification skews
306 the BMR calculation to only include beneficial mutations that were fixed in the population.
307 There is a potential that other beneficial mutations are possible, but were not observed due to
308 either clonal interference or genetic drift (37). As observed in the fitness trajectories for passage
309 sizes of 0.01% and 0.001%, not all experiments were able to make jumps to occupy all the states.
310 For instance, with a passage size of 0.01%, only 4 of 6 experiments were able to make the
311 transition from State 2 to State 3 by experiment's end. In simulation, the same distribution

among the various end states is observed. The distribution observed in simulation is highly dependent on the supply of beneficial mutations captured by the BMR parameter. Thus, the BMR can be fit to yield the same distribution across states as observed experimentally. The BMR was computed using transitions from both State 2 to State 3 and from State 1 to State 2. Since all experiments made the transition from State 1 to State 2, the distribution was used at the day 20 mark where a distribution existed. The 95% confidence interval for the BMR was calculated by fitting the BMR to the 95% confidence interval of the experimental distribution of states. The results yielded a BMR of $10^{-6.9}$ - $10^{-8.4}$ mutations per cell division. The confidence interval was determined by a maximum likelihood estimate as implemented in the binofit function in MATLAB.

Retrospective Validation of ALEsim

ALEsim and the derived parameters (beneficial mutation rate and allowed increases in growth rate) were analyzed using two previously performed ALE experiments on glucose (7, 18) and a legacy experiment on glycerol (14). The outcomes of the two glucose experiments yielded disparate final growth rates despite identical strains and media (*E. coli* K-12 MG1655 in M9 glucose minimal media), 1.00 ± 0.02 with 6 replicates and 0.79 ± 0.01 with 3 replicates, respectively. The only differences between the experiments were three experimental parameters: batch culture volumes (250 mL vs. 25 mL), optical densities when passed (variable vs. OD_{600nm} 1.2), and passage sizes (variable vs. 800 μ L) in the Charusanti et al. (18) and the LaCroix et al. (7) studies, respectively. ALEsim was constrained to allow only the jumps in growth rates observed in these studies and then simulated the expected fitness trajectories for the two different experimental parameters. The only differences explicitly defined in ALEsim were the different batch culture volumes, passage optical densities, and passage volumes. The results showed that

the difference in the final growth rates achieved can be sufficiently explained by the differences in these parameters only (Figure 5). Furthermore, when simulating a legacy dataset for evolving *E. coli* on glycerol minimal media, ALEsim was able to successfully predict that all experiments (n=4) should reach fitness state 3 for the given experimental parameters, as reported in the study (14). The largely different outcome in fitness (i.e., no fitness jumps vs. a significant increase) on glucose, as well as a consistent prediction of fitness on a legacy glycerol dataset, further highlights the importance of properly designing an experiment and validates ALEsim and its parameterization.

ALEsim Applications

Simulations of ALE experiments with the derived beneficial mutation rate and fitness states can enable statements to be made about optimality. The time required to see a given increase in fitness was simulated for a range of increases in growth rate over a range of passage sizes (Figure 6). The results show the average length of time needed to see a measurable change in growth rate due to a beneficial mutation for a range of passage sizes. Figure 6 was derived for growth rate increases that occur from a single mutational event. Based on the passage size and length of time with no increase in growth rate, a conclusion about how close a population is to reaching another state of increased fitness. For example, if a given evolution experiment has achieved a certain growth rate, μ , and has not shown an increase in growth rate with a passage size of 0.1% for 13 days, then there is no likely increase in growth rate available which is greater than 0.10 hr^{-1} from a single mutational event.

Increasing the passage size raises the probability of capturing a beneficial mutation however this also leads to an inflation in the resources needed to sustain the experiment (Figure 6). For example, if an ALE experiment with a passage size of 0.1% were being passed twice a day

(every 12 hours), the same experiment with a passage size of 10% would need to be passed 6 times per day (every 4 hours). The magnitude of resources needed to maintain an experiment tend to scale with each batch. Thus, the more batches needing to be processed, the more media, pipette tips, culture vessels, and labor costs are required. A single person can feasibly do an experiment passed every 12 hours whereas passing every 4 hours would require coordinated effort by multiple persons or an automated platform. Therefore, understanding what is gained with the larger passage size is important before committing to such a large expenditure of resources. ALEsim can quantify the gains or losses achievable with different passage sizes to help identify the ideal experimental setup (Figure 6).

367

368 **Mutation Frequency Analysis by Passage Size**

369 Clones from the endpoint populations of each independent experiment were isolated and
370 resequenced. Two clones showed hypermutating tendencies. This was identified by the number
371 of mutations ($p < 0.01$) and the presence of a mutation in *mutY* or *mutL*. Experiments with larger
372 passage size led to an increase in the number of mutations found. Mutated alleles were therefore
373 grouped by passage size. Clones isolated from larger passage size experiments, on average, had
374 more alleles being selected (Figure 7). Of all mutations identified, those in *glpK* were
375 specifically tracked. Mutations in *glpK* have previously been shown to be causal (with a
376 significant impact on fitness) as well as ubiquitous, mutating more than any other alleles under
377 glycerol growth conditions (14). Thus *glpK* is a good indicator of the how effective the various
378 passage sizes are at fixing beneficial mutations. Consequently, there is a positive relationship
379 between the fixing of *glpK* mutations and the passage size until saturation is reached. With the

380 passage size dropped to the lowest value (0.001%), the observed fraction that fixed was only
381 0.33 (2/6).

382 Discussion

383 The conceptual purpose of an ALE experiment is to move an organism towards a more optimal
384 (fit) state in the presence of a selection pressure. Absolute optimality is difficult, if even possible,
385 to define. It has been shown that even for a laboratory evolution, there is still room for evolution
386 after 50,000 generations (38). The continual ability of organisms to evolve and innovate makes it
387 difficult to analyze the results of an ALE experiment in the context of optimality. What is
388 immediately apparent is that there are diminishing returns. As an ALE experiment progresses,
389 the increase in growth rate or fitness tends to decrease in magnitude (1, 39-43). The smaller
390 increases take longer lengths of time to occur and become fixed in the population
391 (Supplementary Text). Given this property and the desire to understand and leverage the ALE
392 process, ALEsim was built and validated through performing a control experiment. ALEsim was
393 first parameterized with a set of control experiments using different passage sizes.
394 Parameterization revealed a beneficial mutation rate of $10^{-6.9}$ - $10^{-8.4}$ mutations per cell division,
395 consistent with previously reported values and distinct fitness states (27, 28). Validation was
396 then carried out using additional legacy experiments and ALEsim proved sufficient for
397 explaining the differences in observed experimental outcomes (i.e., growth rates) based on the
398 parameters employed in each study (i.e., passage size, passage OD, and culture volume) (Figure
399 5). Lastly, ALEsim was applied to quantify tradeoffs in experimental design considerations for
400 desired outcomes and was used to demonstrate how it can be leveraged for determining the key
401 aspect of experiment termination.

402 The ability to optimize and design ALE experiments is possible with the ALEsim computational
403 framework. Given a certain amount of resources, ALEsim can calculate how best to deploy them
404 at different stages of an experiment to shorten project timelines and achieve desired outputs. For

405 example, near the beginning of the ALE experiments, the increases in growth rates found are
406 typically quite large. Because of this, a large passage size does not have an additional benefit.
407 This is evident in the experiment performed here in that passage sizes of 0.1%, 1%, and 10%
408 mostly reached states 1, 2, and 3A at about the same time (Figure 3). In planning future ALE
409 experiments, the added resource usage needed to maintain an experiment at a 10% passage size
410 does not appear to be justified. However, the added benefits become apparent when looking at
411 the transition from state 3A to 3B. It could then be suggested that if the goal is to get as close to
412 the absolute optimal state as reasonably possible, the added resources of maintaining a 10%
413 passage size experiment only need to be maintained after initial large increases in growth rate or
414 fitness are found. This would not eliminate the difficulty in maintaining such an experiment, but
415 would at least reduce the length of time the experiment would need to be run at such a high
416 resource ‘burn’ rate. With ALEsim, these types of resource/fitness tradeoff analyses can now be
417 calculated and should be leveraged in experimental design. The approach of dynamic resource
418 allocation opens the door for project optimization typical of engineering process design.

419 Knowing the distance to optimality can aid in determining when to terminate an ALE
420 experiment. The typical method of determining when to stop an ALE experiment is to
421 subjectively determine that no more increases in fitness are being observed. However, this
422 approach of waiting to observe a plateau in fitness can be artificial given a small passage size.
423 An example of how this approach can be misleading is the observation that passage sizes of
424 0.1% and 1% showed no increase in growth rate after reaching state 3A for at least 15 days
425 (Figure 3). However, given that slight increases in growth rates beyond state 3A to state 3B with
426 a passage size of 10% were observed, it can be concluded that state 3A is not the optimal state.
427 Thus, if only a 1% passage size was used, the experiment could be terminated before finding

428 state 3B. Further, it would be incorrect to compare experiments with a 10% passage size to a 1%
429 passage size without understanding the context of the effects of the different passage sizes.
430 Perhaps the best example of this is provided through the analysis of legacy ALE experiments
431 (Figure 5). Two experiments with the same strain and media conditions yielded vastly different
432 fitness outcomes. This difference is subsequently explainable within the scope of ALEsim.
433 Therefore, having access to a computational framework such as ALEsim can enable the
434 researcher to make an informed decision about when to terminate an experiment given the
435 capacity and resources of the experimental setup and the desired/acceptable outcome. This type
436 of termination analysis is laid out in Figure 6 and can be calculated *de novo* for any experiment
437 given the current growth rate and passage size. It also should be noted that this type of analysis
438 could result in a standard for the ALE community as one could state the ALEsim generated $\Delta\mu$ at
439 the time of termination.

440 The ability to design and carry out complicated and high resource burn ALE experiments is
441 likely only feasible through automation of the ALE process. Automation was utilized here and in
442 previous studies (4, 7, 44). Manual processes are often hindered by researcher availability
443 whereas machines can measure and pass around the clock (e.g., approximately 5-7 passages per
444 day were performed in automated studies (4, 7, 44), compared to 1-2 per day manually (14, 15,
445 18). Thus, the ability to automate and optimize ALE is likely to accelerate adoption of the ALE
446 experimental technique and broaden the application areas. Furthermore, the ALEsim framework
447 and output can also be used as a basis for modeling much of the legacy data currently available
448 for ALE experiments which include lag, exponential, stationary, and/or stressed phases. As the
449 selection pressure in such experiments is more complex and growth is defined by more than the
450 growth rate parameter (e.g. lag phase duration, stationary phase mutation rate, growth phase

451 transistions, etc...), ALEsim in its current format would have to be expanded. Nonetheless,
452 ALEsim and its parameterization here demonstrates the utility of using simulated design in the
453 ALE process and establishes a portable code base.

454 The field of adaptive laboratory evolution is expanding, largely due to lower costs of next
455 generation sequencing. Innovative applications are appearing and are being applied to a range of
456 organisms (1, 3). This growth in ALE use has occurred without a standard operating procedure
457 for performing and quantifying these experiments. Consequently, this leads to ill-defined
458 endpoints of experiments and the inefficient use of resources. The ALEsim computational
459 platform developed here would provide a basis with which to quantify experiments and aid in
460 their design; matching the desired outcome with resources available.

461

462 **List of Supplementary Files**

463 - Supplemental text (calculations)

464 ○ Supplementary Table – ALE Fitness Stats

465 ○ Supplementary Figure 1 – Sensitivity analysis of dry weight per cell values

466 - Supplementary File 1 – MATLAB m files: ALE Model m-files

467

468

469 **Acknowledgements and Funding Information**

470 This work was supported by the Novo Nordisk Foundation Center for Biosustainability

471 We'd like the Marc Abrams, Troy Sandberg, and Richard Szubin for their assistance with this
472 manuscript.

473

474 **Tables**

475 None

476

477 **Figure Legends**478 **Figure 1 - ALEsim Flow Chart**

479 A workflow outlining the logical steps the simulator takes when performing a single simulated
480 ALE experiment. Due to the stochastic nature of ALE experiments, *in vivo* and *in silico*, multiple
481 experiments are averaged together to identify general trends.

482 **Figure 2 - Governing Equations, Assumptions, and Parameters for ALEsim**

483 a) Microbe growth occurs according to an exponential growth curve where μ is the growth rate, t
484 is the time elapsed, N_0 is the initial cell count at $t=0$, and $N(t)$ is the cell count at a given time, t .
485 No lag phase or stationary phase is modeled. The total cell count ($N(t)$) is determined by the
486 summation of exponential growth curves for all individual cells lines. b) Favorable mutations
487 occur during cell growth according to a binomial distribution where each cell division represents
488 one Bernoulli trial with a probability of success equal to the beneficial mutation rate (BMR). c)
489 Each flask is modeled as a completely homogenous culture. d) The number of cells represented
490 for each cell line in each inoculum is randomly chosen according to a normal distribution with a
491 mean and variance equal to the number of cells represented in the flask, N_{Green}^{Flask} times the ratio of
492 the flask volume, V_{Flask} , to inoculum volume, $V_{Inoculum}$. e-g) The volume of media per flask,
493 inoculum volume, and passage optical density can be altered. h) The simulated ALE experiment
494 can be stopped after a specified amount of time or maximum number of flasks. i) Based on the

relative growth rate increases seen in ALE experiments, a range of allowable growth rate increases is determined. j) Based on matching the evolution trajectory (plot of growth rate vs. flask #) with varying the beneficial mutation rate (BMR), the probability of a favorable mutation is obtained. k) Since each ALE is based on randomly generated mutations, multiple ALE simulations are averaged together to get repeatable results from the same parameters. The number of simulations is user controlled.

Figure 3 – Fitness Trajectory of *E. coli* evolved on Glycerol

The absolute growth rates of independently evolved cultures of *E. coli* as fitted by a cubic spline for all ALE experiments separated by the different passage sizes. Dashed lines represent regions where the spline fit is based on sparse data, and therefore not considered accurate. The small upturn in growth rates at the endpoint is an artifact of the spline interpolation and is ignored when determining endpoint growth rates. All except five ALE experiments reached fitness State 3. The rate at which the final growth rate was achieved varied. The hypermutating strain with a passage size of 10% reached State 3 significantly faster than all others (it possessed a mutation in *mutY*). The purple hypermutating strain was identified as a potential hypermutating strain based on the number of mutations fixed ($p=0.003$, $FDR=0.087$) and the presence of a frame shift insertion in *mutL*.

Figure 4 – Distribution of Fitness Increases in Glycerol ALE

A histogram of the normalized increases in growth rate ($\mu_{\max} = 0.64 \text{ hr}^{-1}$) attributed to each jump for the different experiments. The fitness increases were categorized by which state transition was made. The different passage sizes (indicated by different colors) did not show any significant variance in the ability to fix distinct increases in growth rate. A few small jumps not

517 shown are small observed increases in fitness that did not jump between any of the states
518 identified.

519 **Figure 5 – Simulated vs Experimental Results with Large and Small Passage Sizes**

520 Two ALE experiments of *E.coli* MG1655 in glucose M9 minimal media were simulated using
521 ALEsim. The strain and media conditions were identical in the two experiments. The only
522 differences were in the culture volume (25ml vs. 250mL), optical density when passed (variable
523 vs. 1.2 OD_{600nm}), and passage volume (variable vs 800μL). The variable nature of the optical
524 density when passed and the passage size in the latter experiment was a consequence of
525 manually passing the culture each day. The former experiment employed an automated system of
526 monitoring and passing the culture to maintain consistency. Despite being the same strain and
527 conditions, the final fitness achieved in the two experiments were quite different. ALEsim was
528 used to simulate these same experiments with the only differences being the three
529 aforementioned parameters. Consequently, the ALEsim results showed that the differences in
530 these parameters were sufficient to explain why the final growth rates achieved were different,
531 further highlighting the importance of choosing these parameters properly. The simulated
532 results are represented by a 95% confidence interval. The confidence interval for Experiment
533 #2 is too small to be visible.

534 **Figure 6 – Upper Bound on possible jumps in growth rates**

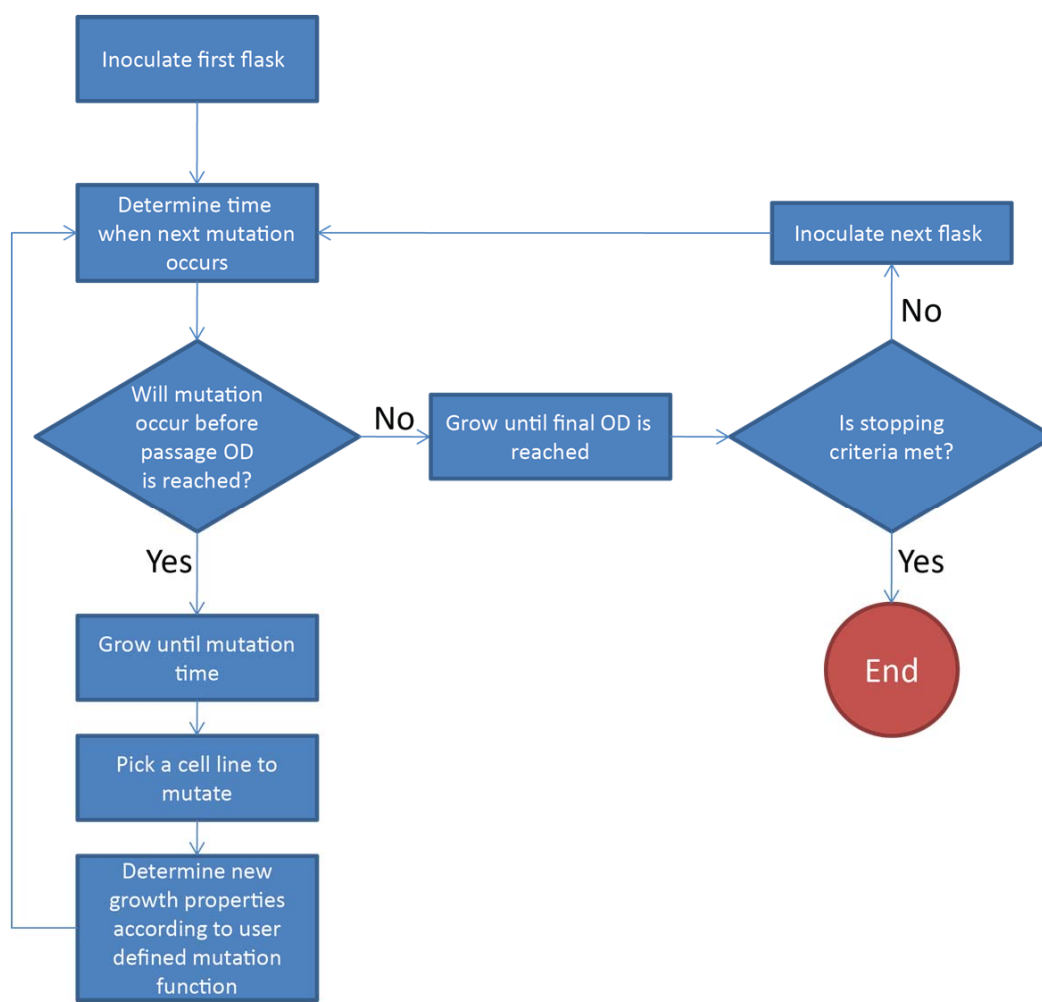
535 A. Upper bounds on possible jumps in growth rates are shown. At a given point in time, a jump
536 that reaches above the upper bound is statistically infeasible (95% confidence) from a single
537 mutation, whereas jumps that stay below the line are possible. B. The upper bound on jumps is
538 shown for varying passage sizes. These experiments were simulated with parameters that

539 matched the experimental parameter used. Increasing the passage size can have a significant
540 impact on the upper bound. Consequently, the time required to eliminate jumps of certain
541 magnitudes can take much longer to achieve. However, as the passage size increases there comes
542 a point when the returns begin to diminish such that passage sizes between 0.1% and 10% did
543 not show a large difference in the time required to find a given jump. C. Relative amount of
544 resources needed to perform an ALE experiment normalized to the lowest passage size. As the
545 passage size is increased the resource usage begins to increase greatly.

546 **Figure 7 – Genetic Analysis – By Passage Size**

547 A bar chart representing the observed fraction of mutations at a given passage volume. As a
548 general trend, the larger the passage size, the greater the probability of a mutation in a given
549 allele fixing in the population. A key mutation in the *glpK* gene is displayed as well as all
550 mutations. The ordinal rank of passage size was compared to the observed fraction of mutations
551 using a Wilcoxon rank test and resulted in p-values of 0.008 and 0.024 for all mutations and
552 *glpK* mutations, respectively.

553

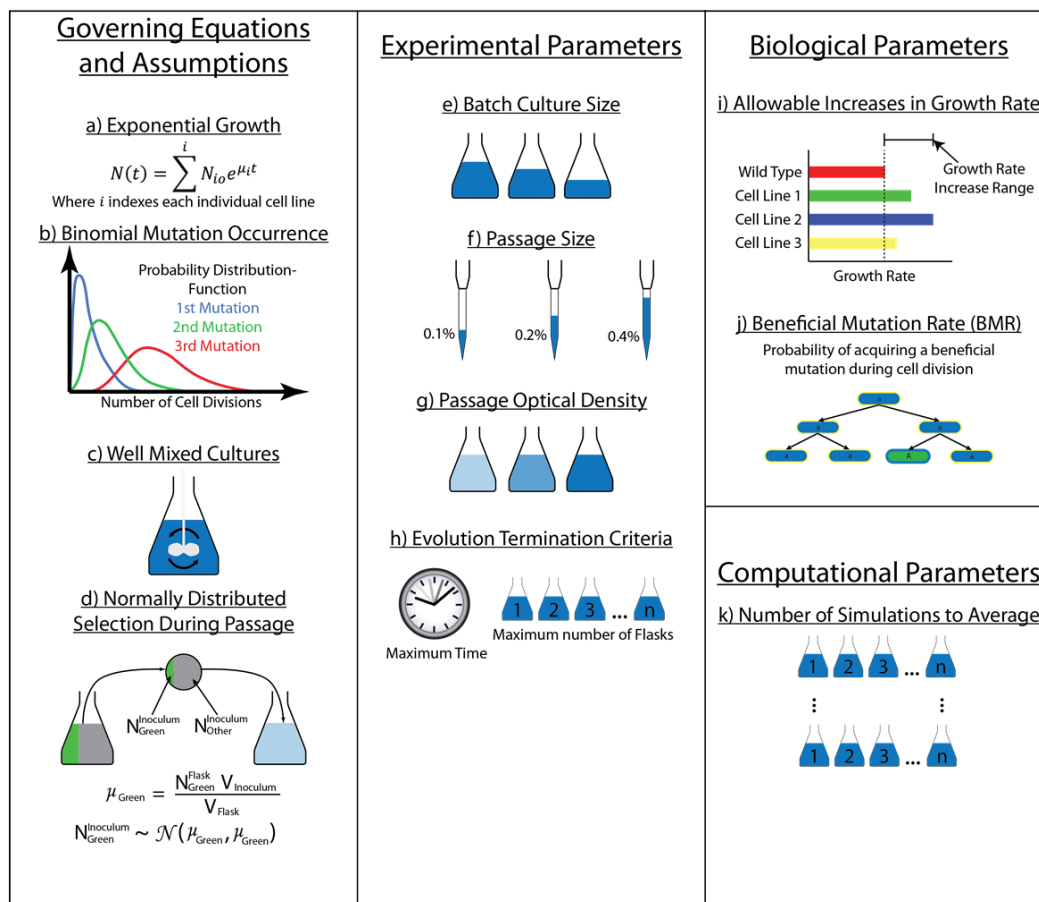


554

555 **Figure 1**

556

557



558

559 **Figure 2**

560

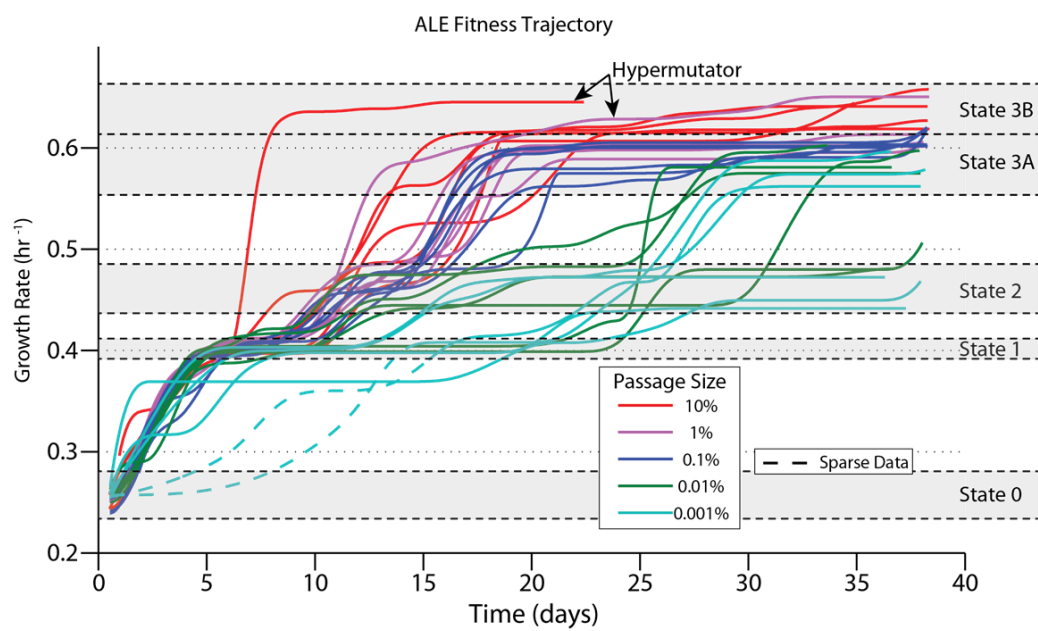
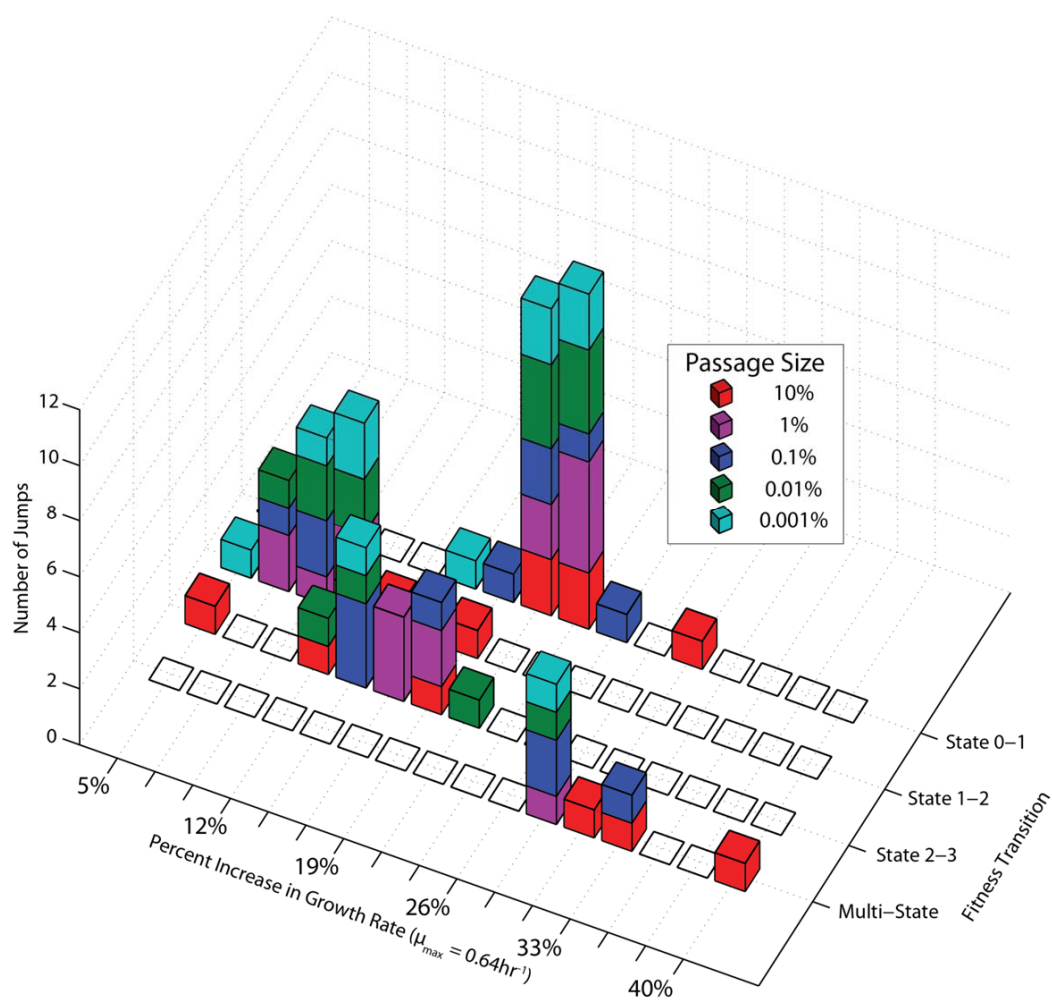


Figure 3



564

565 **Figure 4**

566

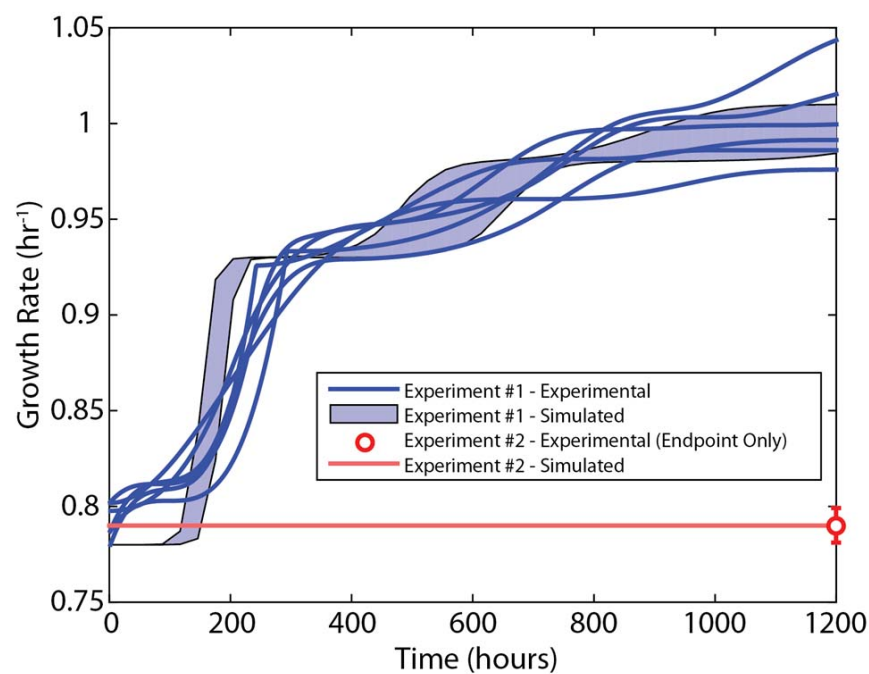


Figure 5

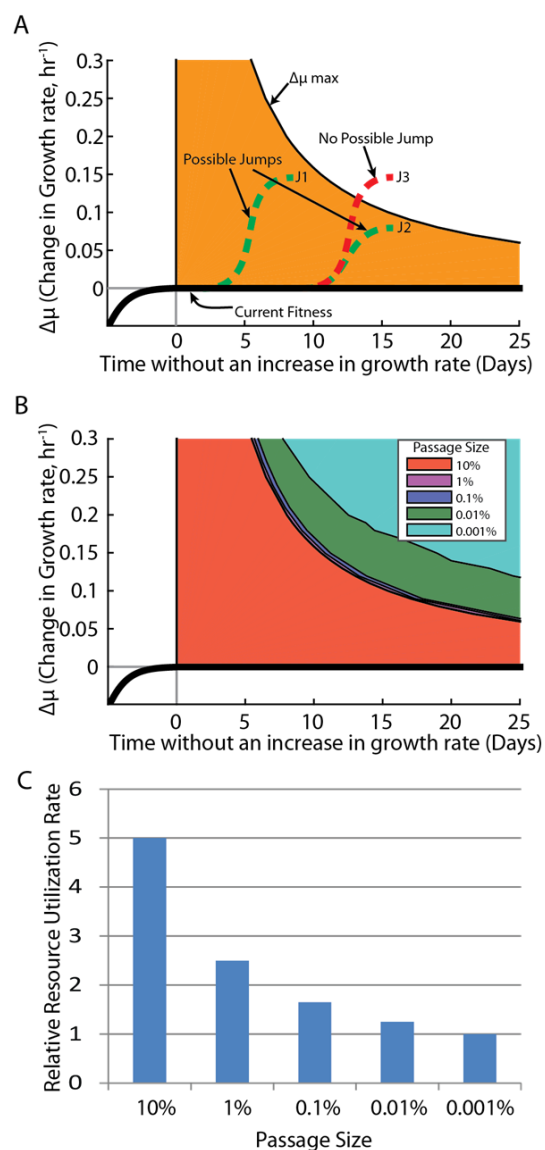
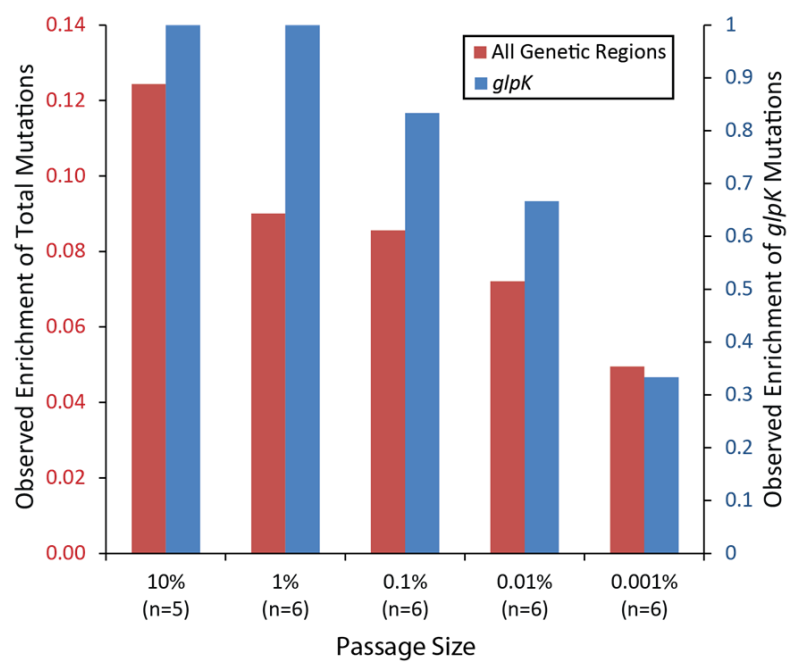


Figure 6



573

574 **Figure 7**

575 **References**

576

- 577 1. **Palsson B.** 2010. Adaptive laboratory evolution. *Microbe*.
- 578 2. **Conrad TM, Lewis NE, Palsson BO.** 2011. Microbial laboratory evolution in the era of genome-
579 scale science. *Mol Syst Biol* **7**:509.
- 580 3. **Dragosits M, Mattanovich D.** 2013. Adaptive laboratory evolution -- principles and applications
581 for biotechnology. *Microb Cell Fact* **12**:64.
- 582 4. **Sandberg TE, Pedersen M, LaCroix RA, Ebrahim A, Bonde M, Herrgard MJ, Palsson BO, Sommer
583 M, Feist AM.** 2014. Evolution of *Escherichia coli* to 42 degrees C and subsequent genetic
584 engineering reveals adaptive mechanisms and novel mutations. *Mol Biol Evol* **31**:2647-2662.
- 585 5. **Harcombe WR, Delaney NF, Leiby N, Klitgord N, Marx CJ.** 2013. The ability of flux balance
586 analysis to predict evolution of central metabolism scales with the initial distance to the
587 optimum. *PLoS Comput Biol* **9**:e1003091.
- 588 6. **Gresham D, Hong J.** 2015. The functional basis of adaptive evolution in chemostats. *FEMS
589 Microbiol Rev* **39**:2-16.
- 590 7. **LaCroix RA, Sandberg TE, O'Brien EJ, Utrilla J, Ebrahim A, Guzman GI, Szubin R, Palsson BO,
591 Feist AM.** 2015. Use of adaptive laboratory evolution to discover key mutations enabling rapid
592 growth of *Escherichia coli* K-12 MG1655 on glucose minimal medium. *Appl Environ Microbiol*
593 **81**:17-30.
- 594 8. **Bacun-Druzina V, Cagalj Z, Gjuracic K.** 2007. The growth advantage in stationary-phase (GASP)
595 phenomenon in mixed cultures of enterobacteria. *FEMS Microbiol Lett* **266**:119-127.
- 596 9. **Vasi F, Travisano M, Lenski RE.** 1994. Long-term experimental evolution in *Escherichia coli*. II.
597 Changes in life-history traits during adaptation to a seasonal environment. *American
598 Naturalist*:432-456.
- 599 10. **Bachmann H, Fischlechner M, Rabbers I, Barfa N, Branco dos Santos F, Molenaar D, Teusink B.**
600 2013. Availability of public goods shapes the evolution of competing metabolic strategies. *Proc
601 Natl Acad Sci U S A* **110**:14302-14307.
- 602 11. **Raynes Y, Halstead AL, Sniegowski PD.** 2014. The effect of population bottlenecks on mutation
603 rate evolution in asexual populations. *J Evol Biol* **27**:161-169.
- 604 12. **Campos PR, Wahl LM.** 2010. The adaptation rate of asexuals: deleterious mutations, clonal
605 interference and population bottlenecks. *Evolution* **64**:1973-1983.
- 606 13. **Campos PR, Wahl LM.** 2009. The effects of population bottlenecks on clonal interference, and
607 the adaptation effective population size. *Evolution* **63**:950-958.
- 608 14. **Herring CD, Raghunathan A, Honisch C, Patel T, Applebee MK, Joyce AR, Albert TJ, Blattner FR,
609 van den Boom D, Cantor CR, Palsson BO.** 2006. Comparative genome sequencing of *Escherichia
610 coli* allows observation of bacterial evolution on a laboratory timescale. *Nat Genet* **38**:1406-
611 1412.
- 612 15. **Ibarra RU, Edwards JS, Palsson BO.** 2002. *Escherichia coli* K-12 undergoes adaptive evolution to
613 achieve in silico predicted optimal growth. *Nature* **420**:186-189.
- 614 16. **Lee DH, Palsson BO.** 2010. Adaptive evolution of *Escherichia coli* K-12 MG1655 during growth on
615 a Nonnative carbon source, L-1,2-propanediol. *Appl Environ Microbiol* **76**:4158-4168.
- 616 17. **Conrad TM, Joyce AR, Applebee MK, Barrett CL, Xie B, Gao Y, Palsson BO.** 2009. Whole-
617 genome resequencing of *Escherichia coli* K-12 MG1655 undergoing short-term laboratory

- 618 evolution in lactate minimal media reveals flexible selection of adaptive mutations. *Genome Biol*
619 **10**:R118.
- 620 18. **Charusanti P, Conrad TM, Knight EM, Venkataraman K, Fong NL, Xie B, Gao Y, Palsson BO.**
621 2010. Genetic basis of growth adaptation of *Escherichia coli* after deletion of *pgi*, a major
622 metabolic gene. *PLoS Genet* **6**:e1001186.
- 623 19. **Wahl LM, Gerrish PJ.** 2001. The probability that beneficial mutations are lost in populations with
624 periodic bottlenecks. *Evolution* **55**:2606-2610.
- 625 20. **Hubbarde JE, Wahl LM.** 2008. Estimating the optimal bottleneck ratio for experimental
626 evolution: the burst-death model. *Math Biosci* **213**:113-118.
- 627 21. **Deatherage DE, Barrick JE.** 2014. Identification of mutations in laboratory-evolved microbes
628 from next-generation sequencing data using breseq. *Methods Mol Biol* **1151**:165-188.
- 629 22. **Neidhardt FC, Ingraham JL, Schaechter M.** 1990. *Physiology of the bacterial cell : a molecular*
630 *approach*. Sinauer Associates, Sunderland, Mass.
- 631 23. **Pramanik J, Keasling JD.** 1997. Stoichiometric model of *Escherichia coli* metabolism:
632 incorporation of growth-rate dependent biomass composition and mechanistic energy
633 requirements. *Biotechnol Bioeng* **56**:398-421.
- 634 24. **Kibota TT, Lynch M.** 1996. Estimate of the genomic mutation rate deleterious to overall fitness
635 in *E. coli*. *Nature* **381**:694-696.
- 636 25. **Fogle CA, Nagle JL, Desai MM.** 2008. Clonal interference, multiple mutations and adaptation in
637 large asexual populations. *Genetics* **180**:2163-2173.
- 638 26. **Tenaillon O, Rodriguez-Verdugo A, Gaut RL, McDonald P, Bennett AF, Long AD, Gaut BS.** 2012.
639 The molecular diversity of adaptive convergence. *Science* **335**:457-461.
- 640 27. **Desai MM, Fisher DS, Murray AW.** 2007. The speed of evolution and maintenance of variation
641 in asexual populations. *Curr Biol* **17**:385-394.
- 642 28. **Perfeito L, Fernandes L, Mota C, Gordo I.** 2007. Adaptive mutations in bacteria: high rate and
643 small effects. *Science* **317**:813-815.
- 644 29. **Gerrish PJ, Lenski RE.** 1998. The fate of competing beneficial mutations in an asexual
645 population. *Genetica* **102-103**:127-144.
- 646 30. **Uecker H, Hermisson J.** 2011. On the fixation process of a beneficial mutation in a variable
647 environment. *Genetics* **188**:915-930.
- 648 31. **Lande R.** 2007. Expected relative fitness and the adaptive topography of fluctuating selection.
649 *Evolution* **61**:1835-1846.
- 650 32. **Wright S.** 1929. Fisher's Theory of Dominance. *American Naturalist* **63**:274-279.
- 651 33. **Haldane JBS.** 1927, p 838-844. *Mathematical Proceedings of the Cambridge Philosophical*
652 *Society*.
- 653 34. **Fisher RA.** 1930. *The genetical theory of natural selection*. The Clarendon press, Oxford,.
- 654 35. **Wahl LM, Zhu AD.** 2015. Survival probability of beneficial mutations in bacterial batch culture.
655 *Genetics* **200**:309-320.
- 656 36. **Foster JA.** 2001. Evolutionary computation. *Nat Rev Genet* **2**:428-436.
- 657 37. **Reyes LH, Almario MP, Winkler J, Orozco MM, Kao KC.** 2012. Visualizing evolution in real time
658 to determine the molecular mechanisms of n-butanol tolerance in *Escherichia coli*. *Metab Eng*
659 **14**:579-590.
- 660 38. **Wiser MJ, Ribick N, Lenski RE.** 2013. Long-term dynamics of adaptation in asexual populations.
661 *Science* **342**:1364-1367.
- 662 39. **Kryazhimskiy S, Rice DP, Jerison ER, Desai MM.** 2014. Microbial evolution. Global epistasis
663 makes adaptation predictable despite sequence-level stochasticity. *Science* **344**:1519-1522.
- 664 40. **Khan AI, Dinh DM, Schneider D, Lenski RE, Cooper TF.** 2011. Negative epistasis between
665 beneficial mutations in an evolving bacterial population. *Science* **332**:1193-1196.

- 666 41. **Chou HH, Chiu HC, Delaney NF, Segre D, Marx CJ.** 2011. Diminishing returns epistasis among
667 beneficial mutations decelerates adaptation. *Science* **332**:1190-1192.
- 668 42. **Barrick JE, Kauth MR, Strelisoff CC, Lenski RE.** 2010. *Escherichia coli* rpoB mutants have
669 increased evolvability in proportion to their fitness defects. *Mol Biol Evol* **27**:1338-1347.
- 670 43. **Perfeito L, Sousa A, Bataillon T, Gordo I.** 2014. Rates of fitness decline and rebound suggest
671 pervasive epistasis. *Evolution* **68**:150-162.
- 672 44. **Sandberg TE, Long CP, Gonzalez JE, Feist AM, Antoniewicz MR, Palsson BO.** 2016. Evolution of
673 *E. coli* on [U-13C]Glucose Reveals a Negligible Isotopic Influence on Metabolism and Physiology.
674 *PLoS One* **11**:e0151130.
- 675
- 676